

## Can Surface Adhesion Drive Cell-rearrangement? Part I: Biological Cell-sorting

FRANÇOIS GRANER†

*Research Institute for Electrical Communications, Tohoku University,  
2-1-1 Katahira, Sendai 980, Japan*

*(Received on 18 August 1992, Accepted in revised form on 26 March 1993)*

We explore the dynamical effects of surface adhesion on biological cell-sorting. We start with the simple idea that cell–cell adhesion is associated with an energy per unit area and define the total adhesion energy as a function of the cell configuration. We discuss whether deterministic cell motion, following the gradient of this position-dependent energy, can successfully explain cell-sorting in biology. We conclude: (i) Adhesion alone could be the source of cell movement. Internal cell activity is not necessary, although not excluded. (ii) For mixtures of two cell types, differential adhesion suffices to make clusters of the more cohesive cells coalesce and round. (iii) The presence of stable or metastable configurations, reached by relaxation of cell–cell adhesion energy, can explain why cell movement stops in biological experiments. (iv) Free boundaries, temperature and cell shapes affect cell-sorting. (v) Adhesion can also drive rearrangement in an homogeneous collection of cells.

### 1. Introduction

What forces drive cell movement during cell-sorting? When cells of two or more types are randomly intermingled and aggregated, they are able to sort and move over long distances compared to their diameter, to re-establish homogeneous cell masses and sometimes to reconstitute functional tissues (for a review, see Armstrong, 1989). The rearrangement of cells plays an essential role in morphogenesis and wound healing. However, the sorting mechanism is still not understood in many cases. Two main questions arise: is the cell movement directed, and if so, how? What force drives cell movement, and how is it generated at the molecular level?

Differential intercellular adhesivity can direct the movement of sorting cells (for a review see Steinberg, 1975; Armstrong, 1989; Newman & Comper, 1990). Many different adhesion mechanisms are possible (Curtis, 1988) including electrostatic interactions (Bell, 1979; Bongrand, 1988), adherent junctions (Nicol & Garrod, 1982; McClay & Ettensohn, 1987) and specific or non-specific adhesion molecules (e.g. Edelman & Thiery, 1985; Bell, 1988; Fischer, 1991; Takeichi, 1991).

Gustafson & Wolpert (1963) have compared adhesion molecules to the teeth of a zipper which hold two surfaces together. However, we do not know what brings surfaces into initial contact (Fristrom, 1988). Several physical mechanisms are possible (Newman & Comper, 1990). The current favorite is that adhesion can not

† Present address: Laboratoire de Physique Statistique, Ecole Normale Supérieure, 24 rue Lhomond, 75005 Paris, France.

move cells by itself: it only helps to select the most favorable configuration amongst the different possibilities explored by the cells (Steinberg, 1963, 1964, 1970). Thus each cell must actively explore its neighborhood (Oster, 1984; Oster & Perelson, 1987), using protrusions (Jacobson *et al.*, 1986; Armstrong, 1989) and contractions (Phillips & Davis, 1978; Keller & Hardin, 1987; Weliky & Oster, 1990). However, it is not clear whether amoebal movements are necessary for cell-sorting: they could sometimes be an effect of other forces acting on the cell (Steinberg & Wiseman, 1972; Kolega, 1986).

We define "active" or "internal" *motility* as the ability of a single cell to move autonomously using cytoplasmic components, such as actin micro-filaments. We investigate whether even cells lacking locomotive apparatus can have a passive *mobility* and undergo cell-sorting due to "adhesion", a property of the external surface of the cell.

Intuitively, how does a force arise from adhesion? We have to think at the nanometer level. The erratic thermal micro-fluctuations of two cell surfaces can bring them in contact, explore various configurations and stay longer in the more favorable ones. Even when the main contribution to adhesion comes from discrete molecular sites, we can define the adhesion energy and its gradient on a micrometer length scale, at which the discrete fluctuations average. This will be the main point of the present article. Our discussion is qualitative and does not aim to provide a definitive explanation of biological observations; instead we suggest that cell adhesivity should not be ignored as a mechanism. We present elsewhere (Part II, Graner & Sawada, 1993) a more formal geometrical model, along with numerical simulations: it shows how such a force deriving from an energy gradient can make passive viscous cells move over many cell diameters within hours.

We employ three ideas from the biological literature. Hypothesis 1: cells can follow an energy gradient in the absence of other motility mechanisms (Steinberg, 1962; Childress & Percuss, 1981; Oster *et al.*, 1983). Hypothesis 2: cell-cell contact is associated with an adhesion energy per unit of contact area (Thompson, 1942; Lewis, 1948; Steinberg, 1963). Hypothesis 3: the actual geometry of the cells determines the rules by which cells exchange positions (Honda, 1983; Sulsky *et al.*, 1984).

Section II synthesizes and formalizes these ideas. We stress the importance of the cell surface, the topology of neighbors, and the boundaries of the cell aggregate. We link microscopic adhesion mechanisms to the mesoscopic cells by defining surface energies, and to the macroscopic aggregate by defining surface tensions. Section 3 focuses on cell-sorting, with particular attention to metastable configurations and temperature. Section IV discusses differences between cell-sorting and the demixion of fluids.

## 2. Energy and Dynamics

### 2.1. SURFACE ENERGY, DEFINITION AND NOTATION

Confusion arises in the literature concerned with differential cellular adhesion, between terms (for example, free energy, surface free energy, reversible work, work of

adhesion or cohesion, binding strength, adhesion force, surface tension, energy per unit area, affinities) and their corresponding notations (for example,  $e$ ,  $E$ ,  $F$ ,  $W$ ,  $\Delta W$ ,  $\lambda$ ,  $T$ ). We propose a set of coherent definitions.

### 2.1.1. Surface adhesion free energy

Evans (1985, 1988) showed that two cells can repeat contact and separation cycles without hysteresis only if the adhesion is due to continuous mechanisms; or to discrete links, if their average spacing is not too large compared to the link length. They also must be labile, so that they reversibly attach or detach during cell rearrangement. If so, adhesion is uniform on the length scale of a few hundred ångströms. The adhesion free energy  $F(A) - F(0)$  is the integrated mechanical work between the attached state, with a contact area  $A$ , and the separated state, even if non-specific repulsion creates an energy barrier between both states (Bell, 1988).

We define the adhesion free energy per unit of contact area (or "surface free energy" for short) as  $\partial F/\partial A$ . For sticky cells it is negative:  $F$  decreases when cells adhere. It is zero for non-adhesive surfaces, for example, the apical surface of some epithelial cells (Roberson *et al.*, 1980; Armstrong, 1989). It is negative for repulsive surfaces, for example, if they are electrostatically charged (Born & Palinski, 1985). We similarly define a surface free energy with the external medium, (for example, liquid, air, substrate, extracellular matrix or another tissue, Davis, 1984; Bongrand, 1988). A universal theoretical prediction of the surface free energy is not possible. However, Bell (1979, 1988) estimated the contribution of discrete links as a function of their density and mobility.

In principle, experiments can measure this surface free energy (Bongrand, 1988; Curtis & Lackie, 1991). Direct measurements of the cell-cell interaction as a continuous function of  $A$  are possible for red blood cells (Evans, 1980; Evans & Buxbaum, 1981). This method is sensitive to the constitutive relation of the cells (i.e. the relation between a force and the resultant displacement or deformation), especially to membrane elasticity and fluctuations. It is thus more difficult to apply to arbitrary cells (Evans, 1988).

In practice, care is necessary to distinguish the relevant length-scale and time-scale (McClay *et al.*, 1981). Contact forces and long-range interactions between membranes act at different lengths (Evans & Metcalfe, 1984). Membrane roughness is different on 1 nm, 0.1  $\mu\text{m}$  and 1  $\mu\text{m}$  scales (Foa *et al.*, 1988). Physical interactions are instantaneous. Chemical links need from a few seconds to minutes to form (Bell, 1978; Capo *et al.*, 1982, Mège *et al.*, 1986). Adherens junctions and desmosomes need longer. Glazier (private communication) suggests that gentle adhesion-separation cycles could yield AC measurements, with a time scale smaller than the diffusion time of specific receptors (Bell, 1988).

### 2.1.2. Total adhesion energy

For many cells, we need a coarse-grained description to avoid the detailed degrees of freedom arising at scales smaller than the cell size  $R \sim 10^{-3}$  cm (Foa *et al.*, 1988). At larger scales, we can lump in a single effective surface energy  $e$  the microscopic

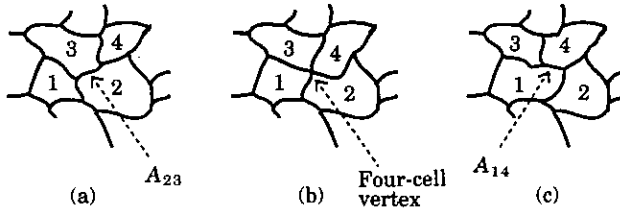


FIG. 1. Sketch of neighbor exchange in two dimensions; for actual observations see Honda *et al.* (1982), Keller & Hardin (1987), Keller & Trinkaus (1987), and for a review Fristrom (1988). (a) Cells 2 and 3 are separating, 1 and 4 approach. The membrane  $A_{23}$  shortens, the vertices 1.2.3 and 2.3.4 approach. (b) By continuity, the vertices 1.2.3 and 2.3.4 fuse to form a transient four-cell vertex; the membrane  $A_{23}$  disappears. (c) The cells still move continuously: 2 and 3 separate, 1 and 4 touch. A new membrane  $A_{14}$  and two new vertices 1.2.4 and 1.3.4 appear, replacing  $A_{23}$ , 1.2.3 and 2.3.4.

entropy contributions to the free energy, arising from the arrangement of surface molecules. For instance, the term  $e$  can include fluctuations in the membrane area. If the actual average contact area  $\mathcal{A}$  between two cells is greater than the apparent one  $A$ , the contact energy  $e\mathcal{A}$  can be written  $e'A$ , with a renormalized surface energy  $e' = (\mathcal{A}/A)e$  greater than the naked one, and the standard deviation of the fluctuation adds a random component to  $e'$ .

Since the configuration entropy is negligible, the configuration energy is equivalent to the free energy (section 3.2.1). The total adhesion energy  $E_{\text{adh}}$  associated with a given configuration can be written as a sum over cells  $i = 1, \dots, N$ , or over the pairs  $(i, j)$  each counted only once:

$$E_{\text{adh}} = \sum_i \left[ \sum_j A_{ij} \frac{e_{ij}}{2} + A_{iM} e_{iM} \right]. \quad (1a)$$

$$= \sum_{(i,j)} A_{ij} e_{ij} + \sum_i A_{iM} e_{iM}, \quad (1b)$$

where  $A_{ij}$  denotes the contact area between cells,  $A_{iM}$  the contact area with the external medium and  $e_{ij} = e_{ji}$ ,  $e_{iM}$  the surface energies associated with these interfaces (Fig. 1). Without free boundaries, for example with periodic boundary conditions, the last term disappears:

$$E_{\text{adh}} = \sum_i \sum_j A_{ij} \frac{e_{ij}}{2} = \sum_{(i,j)} A_{ij} e_{ij}. \quad (2)$$

For a heterogeneous mixture of two cell types, say "dark" ( $d$ ) and "light" ( $l$ ) cells, the energies per unit of interface area,  $e_{ij}$  and  $e_{iM}$ , take the five values  $e_{dd}$ ,  $e_{dl}$ ,  $e_{ld}$  and  $e_{dM}$ ,  $e_{lM}$ . For a homogeneous collection of dark cells they reduce to  $e_{dd}$  and  $e_{dM}$ . Their units are  $\text{erg.cm}^{-2}$ ,  $\text{dyn.cm}^{-1}$  or  $\text{g}^{-2}$ . For a cell monolayer it is convenient to write the contact area  $A_{ij}$  as the product of the contact length  $L_{ij}$  with the cell contact height  $h_{dd}$ ,  $h_{dl}$  or  $h_{ll}$  (which are not necessarily equal, Steinberg & Garrod, 1975; Childress & Percuss, 1981) and to introduce the two-dimensional energies per unit length  $h_{dd} \cdot e_{dd}$ ,  $h_{dl} \cdot e_{dl}$ ,  $h_{ll} \cdot e_{ll}$ , expressed in dynes (Fig. 2).

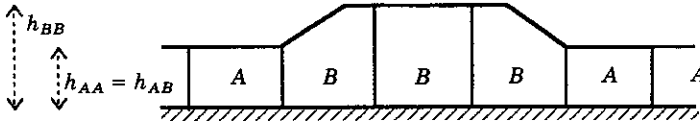


FIG. 2. Cross-section of a cell monolayer on a substrate. The monolayer can be treated as two-dimensional, provided the height of cell-cell contacts  $h_{ij}$  is incorporated into the surface energy  $e_{ij}$  to yield an effective perimeter energy  $h_{ij} \cdot e_{ij}$ .

2.1.3. Surface tensions

We can rewrite eqn (1) to stress its physical content. For instance, by introducing  $\hat{e}_{ij} = e_{ij} - e_{iM} - e_{jM}$  we emphasize the difference in energy between a cell-cell interface and a contact with the medium:

$$E_{adh} = \sum_{(i,j)} A_{ij} \hat{e}_{ij} + \sum_i A_i e_{iM}, \tag{3}$$

where  $A_i$  is the total area of the  $i$ -th cell. If boundaries are homogeneous, as for an aggregate suspended in a liquid medium, and if  $A_i$  is fixed, i.e. each cell area is quasi-incompressible, the last term is constant during an experiment. Then, the dynamics are independent of additive constants in the adhesion energy, and become a function of cell-cell contacts only:

$$E_{adh} = \sum_{(i,j)} A_{ij} \hat{e}_{ij}. \tag{4}$$

For a heterogeneous aggregate of two cell types  $d$  and  $l$ , we can rewrite eqn (1) in terms of macroscopic quantities summed over all the cells:

$$E_{adh} = \left( e_{dM} - \frac{e_{dd}}{2} \right) \sum_{d \text{ cells}} A_{iM} + \left( e_{lM} - \frac{e_{ll}}{2} \right) \sum_{l \text{ cells}} A_{iM} + \frac{e_{dd}}{2} \sum_{d \text{ cells}} A_i + \frac{e_{ll}}{2} \sum_{l \text{ cells}} A_i + \left( e_{dl} - \frac{e_{dd} + e_{ll}}{2} \right) \sum_{\text{contacts } dl} A_{ij}. \tag{5}$$

Introducing the total interfaces areas  $I_{dM}$ ,  $I_{lM}$  and  $I_{dl}$  and their associated energy costs, yields the three surface tensions:

$$\gamma_{dl} = e_{dl} - \frac{e_{dd} + e_{ll}}{2}; \tag{6a}$$

$$\gamma_{dM} = e_{dM} - \frac{e_{dd}}{2}; \tag{6b}$$

$$\gamma_{lM} = e_{lM} - \frac{e_{ll}}{2}; \tag{6c}$$

$$E_{adh} = \gamma_{dM} I_{dM} + \gamma_{lM} I_{lM} + \gamma_{dl} I_{dl} + \sum_{\text{all cells}} A_i \frac{e_{ii}}{2}. \tag{7}$$

The last term, corresponding to the total cell area, is constant in time if each cell area is fixed. These surface tensions  $\gamma$  must not be confused with each membrane's internal tension. They represent the difference in energy between an heterotypic interface and the homotypic interface, per unit area of membrane. These relative costs do not change if a given constant is added to  $e_{ij}/2$  and  $e_{iM}$ :  $\gamma_{iM}$  is the same for attractive cells and repulsive cells in a less favorable medium. Surface tensions are expressed in terms of surface energies, and so carry less information. However, when positive, they are useful intuitive guides; tensions tend to decrease interface areas and smooth out curvatures.

## 2.2. STABILITY

Equilibrium shapes and stationary states are part of descriptive biology; analogies with soap froths, or other physical cellular patterns in metallic grain boundaries, convection or magnetic compounds are fruitful when the concept of minimal surface energy applies. Such analogies early stressed (Boyle, 1660; Hooke, 1665; van Leeuwenhoek, 1692) how minimization of surface energy could determine the equilibrium shape and configurations of cells within various epithelial tissues (Thompson, 1942; Lewis, 1948; Glazier, 1989).

On the other hand, morphogenesis and cell rearrangement deal with changes in time and are different from these physical systems whose cells are unstable. The reason can be sketched as follows. In the total energy  $E_{\text{total}} = E_{\text{adh}} + E_{\text{others}}$  of a cellular pattern, we consider the surface energy term  $E_{\text{adh}}$ . We can classify the degrees of freedom into (i) dilatation, (ii) translation of the cell positions, and (iii) cell shape (which includes all the remaining degrees of freedom).

Let all the dimensions be multiplied by a dilatation coefficient  $\lambda$ :  $A$ , and  $E_{\text{adh}}$ , are multiplied by  $\lambda^2$ ; thus  $dE_{\text{adh}}/d\lambda$  is never zero. Most dynamical studies of physical cellular patterns deal with this instability. In our examples, the contact between two domains is energetically costly ( $e_{ij} > 0$ ). Since domain areas are not constrained, minimizing the total energy leads to decreasing surface area by disappearance of entire domains (Glazier & Weaire, 1992).

In biological patterns a constraint on cell size stabilizes cells and introduces a characteristic length scale (note that the adhesive nature of the contacts usually leads to  $e_{ij} < 0$ , but has no effect on stability). In physics, Bénard-Marangoni convection patterns (Chandrasekhar, 1961; Vélarde & Normand, 1980) are similarly stabilized by the capillary length and are thus analogous to homogeneous biological patterns. An artificial example, the rubber band network (Honda, 1983) constrained both in size and position, undergoes only shape relaxation. Magnetic bubbles in a film may be the only physical analog of heterogeneous biological patterns; they relax in shape and configuration under effect of differential surface energy, but the competition between bulk and wall energy determines their size (Weaire *et al.*, 1991).

For soap froths, the constitutive relation imposes no separate constraints on the area of each bubble. However, biological cells have an elastic surface and bulk compressibility. Cell membranes do not merge during rearrangement, except for rare exchanges of finite quantities of membrane components. The constitutive relations of

biological cells determine the stability against disappearance through  $E_{\text{others}}$ . They are very complex, for example, the cytoskeleton regulates the membrane rigidity and causes anisotropy. Viscosity and elasticity also depend on the time-scale of the applied forces (Phillips & Steinberg, 1978).

2.3. FORCES

The existence of a typical length, for instance the average cell radius  $R$ , allows us to distinguish two separate scales: a microscopic scale much smaller than  $R$ , and a macroscopic one to deal with the topology of the cell configurations. Defining an effective surface energy is a useful way to condense the complexity of actual membranes into a single quantity relevant at macroscopic length scale. The configuration of the network is labeled, at the macroscopic level, by the positions  $\vec{r}_i$  of characteristic topological "objects"; and we can freely choose to think in terms of either vertices, membranes or cell centers (Glazier *et al.*, in preparation). The total surface energy  $E_{\text{adh}}$  depends only on the relative positions of the objects, i.e.  $r_{ij} = |\vec{r}_j - \vec{r}_i|$ . Thus it behaves like a *potential energy* for the cell collection, being invariant under spatial translation and rotation as well as  $i-j$  exchange.

The potential energy governs the system's dynamics because of its position dependence. The energy gradient with respect to the position  $\vec{r}_i$  of each object  $i$ :

$$\vec{\nabla}_i E_{\text{adh}} = \frac{\partial E_{\text{adh}}(\vec{r}_1, \dots, \vec{r}_i, \dots)}{\partial \vec{r}_i} = \sum_j \frac{\partial E_{\text{adh}}(r_{12}, \dots, r_{ij}, \dots)}{\partial r_{ij}} \frac{\vec{r}_{ji}}{r_{ji}} \tag{8}$$

determines the object velocity  $d\vec{r}_i/dt$ . The potential energy  $E_{\text{adh}}$  is physically equivalent to the *force*  $\vec{F}_i = -\vec{\nabla}_i E_{\text{adh}}$  which derives from it.  $\vec{F}$  is the gradient of the total energy; cells move in order to minimize the total energy, not their own energy.

The cell rearrangement literature often mentions this gradient descent. Biological cell adhesion results in surface energy, and is able to drive and direct the rearrangement of cell shapes and positions. Nothing else is required for cell movement, although cell activity increases the mobility.

Therefore a cell need not actively explore its neighborhood. The long-range energy gradient, or force, affects even a cell which does not extend protrusions to its next nearest neighbors, contradicting the intuition that a physical body can not "guess" it could lower its energy by moving to another place.

In the Newtonian notion of force, when an apple falls, there is no point discussing how it knows its energy would be lower on the floor [Fig. 3(a)]. The problem of locally defining and exploring the derivative of the energy is relevant only to the apple's atoms, and is hidden at the observation length. For cells the microscopic fluctuations are apparent on length scales only  $10^2$  to  $10^4$  smaller than the cell size, so the averaging is simpler for continuous adhesion mechanisms (Curtis, 1988) than for discrete ones. Since there is no fundamental difference between gravitational potential energy and adhesive potential energy, apple and cells, like any physical body, both follow the force deriving from the potential energy gradient [Fig. 3(b)].

It is important to note that  $E_{\text{adh}}$  is indeed a continuous and differentiable function of all the space variables  $\vec{r}_i$ , thus its gradient is actually defined. The discrete

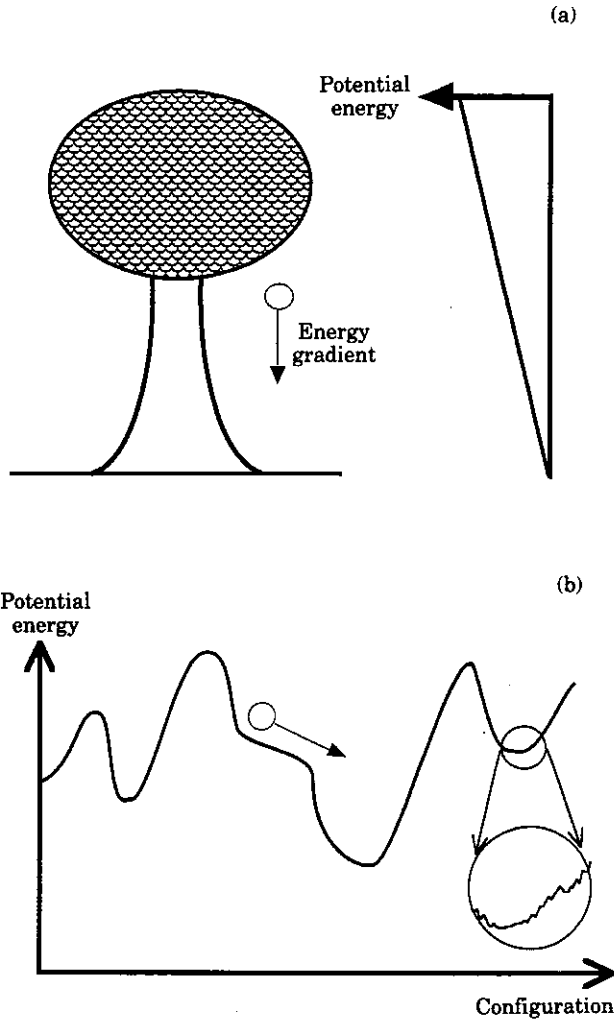


FIG. 3. Forces derived from a gradient. (a) In the Newtonian formalism, the apple accelerates along the gradient of its gravitational potential energy. “Energy gradient” and “force” are complementary and equivalent notions. (b) Sketch of an energy landscape. Like the apple, the whole cell configuration can be passively driven by the force deriving from the gradient of its potential energy. The only necessary condition is that the cells feel a smooth adhesion energy gradient. This occurs if the adhesion agents are continuous, i.e. small and dense, on an observation length scale much smaller than the cell size. If so, the roughness of the energy landscape is hidden on a microscopic scale (enlargement).

summation over each cell  $i$  should not lead to confusion: similarly, when a few bodies interact gravitationally, their interaction potential energy

$$E(\vec{r}_1, \dots, \vec{r}_i \dots) = \sum_{i,j} (Gm_i m_j / r_{ij})$$

yields a force  $\vec{F}_i = -\partial E / \partial \vec{r}_i$  acting on the  $i$ -th body.

2.4. DYNAMICS

Force is a useful concept when we are dealing with non-conservative macroscopic systems and want to avoid the complexity of microscopic degrees of freedom. A cell aggregate is highly dissipative and its viscosity always dominates inertia†. Thus, for instance for one cell, the equation of motion is:

$$\frac{d\vec{r}_i}{dt} = \frac{1}{\mu_c} [-\vec{\nabla}_i E_{adh} + \vec{F}_{others}], \quad (9)$$

where  $\mu_c^{-1}$  is the cell mobility, and  $\vec{F}_{others}$  are all forces not arising from surface adhesion. In the abstract space labeled by the  $N$  positions  $\vec{r}_i$  we can think of the function  $E(\vec{r}_1, \dots, \vec{r}_N)$  as an energy landscape, with hills, saddle points and minima [Fig. 3(b)]. Cells move along the gradient in this abstract multidimensional space, which is not equivalent to a movement along a substrate with an adhesivity gradient in the real space (Carter, 1967).

Equation (9) is deterministic: a given initial condition leads to a single result. The local slope of the landscape makes the global pattern relax towards local minima. Viscosity dissipates all the potential energy. Multiplying the dissipation or dividing all the energies by a constant, changes the time-scale but not the sequence of events (Graner & Sawada, 1993).

3. Cell-sorting

We now study the energy landscape to see if it accounts for observed cell-sorting. Heterotypic cell systems, especially mixtures of two types of cells, have interesting morphogenetic movements during tissue organization. Besides describing these processes, we can investigate the stability of the organization by *in vivo* wounding or *in vitro* reaggregation. Researchers following Holtfreter (1944, 1947) have found cell-sorting in invertebrates and vertebrates, and for embryonic as well as adult cells (reviewed in Armstrong, 1989). Most cases involve separation of the two cell types and the formation of homogeneous tissues, one surrounding the other (Steinberg, 1970). Regeneration of aggregates into living organisms occurs in sponges (Wilson, 1907), sea urchins (Giudice, 1962) and starfish (Dan-Sohkawa *et al.*, 1986); the most striking example being adult hydra which regenerates a normal animal (Noda, 1971; Gierer *et al.*, 1972). In these examples the formation of an epithelial bilayer, surrounding a cavity, is a key step.

† The cell radius  $R$  and speed  $c$  can be as big as  $10^{-3}$  cm and  $10^{-4}$  cm sec<sup>-1</sup> for hydra cell aggregates (Sato & Graner, unpublished data) but  $c$  is much smaller in intact tissues such as natural embryos. The viscosity of a cell collection is much higher than that of the water,  $\nu = 10^{-2}$  cm<sup>2</sup> sec<sup>-1</sup>. Thus, the dimensionless Reynolds number  $Re = cR/\nu$  is less than:

$$10^{-3} \times 10^{-4} / 10^{-2} \sim 10^{-5}$$

and might in fact be  $10^5$  or  $10^8$ – $10^{10}$  times smaller, if the viscosities estimated by Evans (1983) or Gordon *et al.* (1972) are correct. See also Phillips & Steinberg (1978), Purcell (1977), Odell *et al.* (1981), Sulsky *et al.* (1984), Graner & Sawada (1993).

## 3.1. DIFFERENTIAL ADHESION

3.1.1. *Steinberg's hypothesis*

In his differential adhesion hypothesis (DAH) Steinberg made two basic assumptions (e.g. Steinberg, 1962, 1963, 1964, 1970, 1975). DAH1: any contact between two cells has an adhesion energy  $e$  depending on the cell types only. DAH2: cells are mobile enough that they can reach a global energy minimum configuration, independent of initial conditions.

We define dark cells as more cohesive than light cells if  $e_{dd}$  is smaller, or more negative, than  $e_{ll}$ . Is there a hierarchical classification of cells with a single quantitative energy scale (Steinberg, 1970; McClay & Etensohn, 1987)? This energy is not easy to measure, but Steinberg hinted that it should be proportional to the contact area (Steinberg, 1963), our Hypothesis 2. Both perturbing embryos during their development and defining relative scales of cohesiveness in aggregates, show that DAH1 applies to a wider collection of experimental cases than the main competing hypotheses (Thomas & Yancey, 1988; Armstrong, 1989; Friedlander *et al.*, 1989).

Although checked in cell-sorting experiments, DAH2 may be not so universal. In the most common case, called "perfect" cell-sorting, less cohesive light cells surround a round cluster of more cohesive dark cells. Cases of "position reversal" occur, where dark cells surround light cells (Garrod & Steinberg, 1973; Armstrong & Armstrong, 1984). In contrast, "partial" cell-sorting ends with more than one final cluster: experimentally, when an aggregate is made from many more light than dark cells, the latter leave separated islands in the middle of a light cell mass (Steinberg, 1975; Sulsky *et al.*, 1984). Steinberg (1962, 1975) stressed that when cells are not in 1 : 1 proportion, the final state depends on the size-volume ratio as well as the initial geometry of the aggregate.

Differential adhesion can explain both partial cell-sorting and position reversal. DAH is equivalent to a *static* prediction of the minimum energy state. Most of the early numerical simulations of DAH (reviewed in Steinberg, 1975; Sulsky *et al.*, 1984) were also static. Steinberg stressed the importance of dynamic studies, insisting that the minimum energy static equilibrium could be reached only if the cells were mobile enough (Steinberg, 1970, 1975; Gordon *et al.*, 1972). A true dynamic prediction should include three factors, beside the time evolution. (i) Boundaries, usually with the medium, can affect both the evolution and the final state. (ii) Limited cell mobility can prevent cells from ergodically exploring all possible configurations. If so, (iii) the initial conditions determine which local energy minimum is reached.

3.1.2. *Effect of surface energies on cell mobility*

Surface energies usefully describe the neighborhood of a single cell. During a neighbor exchange, two cells separate while two others come into contact [Fig. 4(a)]. From an  $l-l$  contact to an energetically more favorable  $d-d$  one, cells must form a transitory four-cell vertex. If heterotypic contacts are too costly relative to homotypic ones, i.e.  $e_{dl}$  is much higher than  $e_{ll}$ , neighbor exchange can occur only by overcoming an energy barrier [Fig. 4(b)]. On the opposite, if  $e_{dl}$  is much lower than

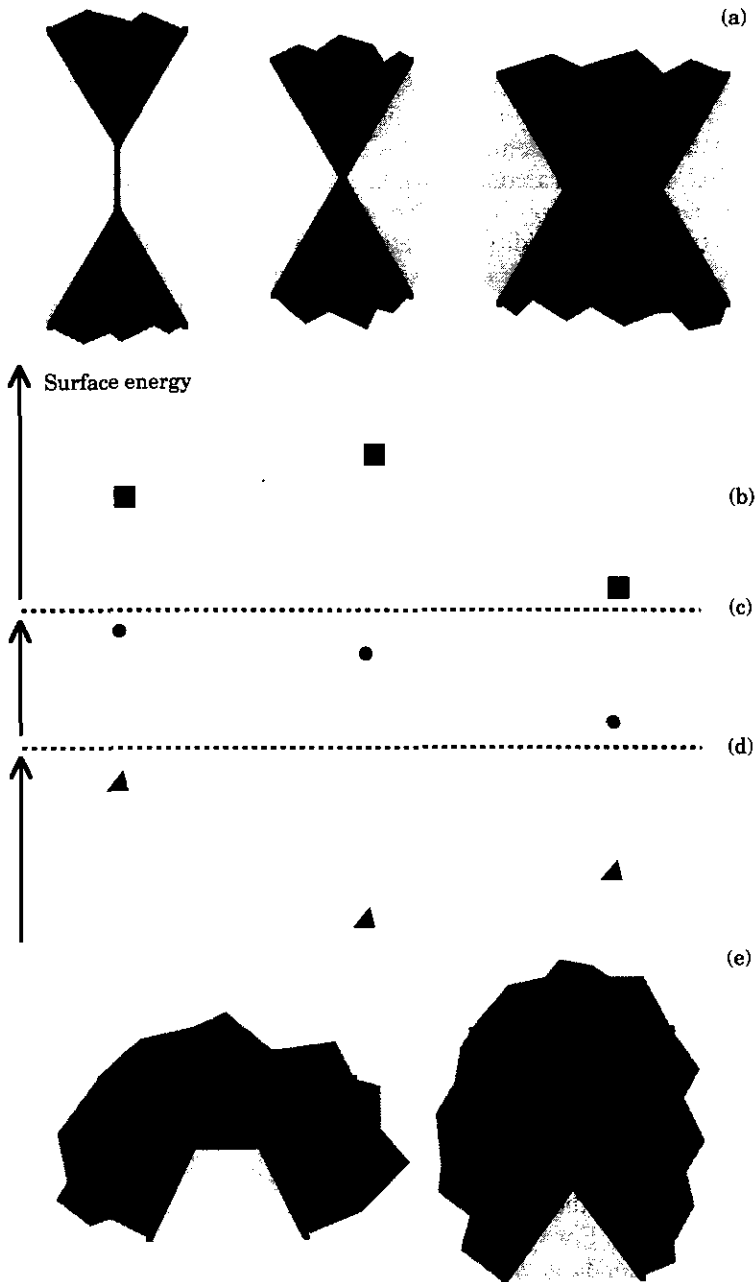


FIG. 4. Two-dimensional cell-sorting by neighbor exchange; see Graner & Sawada (1993). (a) Continuous transition between an initial state and a lower energy state involving a transitory four-cell vertex. "Dark" cells are more cohesive than "light" ( $e_{dd} < e_{ll}$ ). (b)–(d) The intermediate stage has a greater length of heterotypic contact. Depending on the relative surface energies, there can be an energy barrier, i.e. the initial state is metastable (b), a decrease, i.e. the initial state is unstable (c), or a local minimum, i.e. dark and light cells mix (d). (e) Clusters of cohesive cells can condense by expelling other cells.

$e_{dd}$ , the intermediate state is favorable even though it has a greater length of heterotypic contacts, and cells intermingle [Fig. 4(d)].

Between these extremes, energy decreases monotonically in the transition from an  $l-l$  contact to a  $d-d$  one [Fig. 4(c)] and three dark cells can expel a light cell [Fig. 4(e)]. More precisely, contact angles adjust so that any infinitesimal displacement of the vertex causes a second-order variation of the surface energy; but during a neighbor exchange the energy must decrease from a finite amount over a small but finite length, typically the rigidity correlation length of the cell. If the initial density of dark cells is high enough, dark clusters grow by coalescing, percolate and only one final cluster forms. The initial distribution of dark cells around it determines the final size of a cluster. While dark and light cells play a symmetrical role, to the observer the more cohesive dark cells appear to lead the cell-sorting; analogous observations have also been made on *Hydra* regeneration of tissue fragments (Rella, 1941) or recombination of intact ectoderm and endoderm tissues (González, 1985), separated after the mesoglea has been destroyed (Smid & Tardent, 1982).

Three situations favor partial cell-sorting: an initial inhomogeneity in dark cell distribution, a proportion of dark cells much smaller than one half, and a large aggregate. Flat aggregates, especially monolayers (Nicol & Garrod, 1979) are more subject to partial sorting. The relevant quantity is the largest dimension  $L$  of the aggregate, compared to the average cell diameter  $2R$ . If  $L/R$  is much greater than 1, spontaneous coalescence of clusters is impossible when the proportion of dark cells is below a percolation threshold. However, sorting is enhanced if cells are motile, and under thermal agitation (section 3.2.2).

Cell-sorting between endodermal and ectodermal epithelial cells in *Hydra* occurs for up to  $10^6 \sim 10^7$  cells, 15–20% epithelial, even though a normal hydra has around  $10^5$  cells. For more cells, cell-sorting is partial unless the initial aggregate is a long, thin tube in which cells sort radially (Gierer *et al.*, 1972). Thus cell-sorting occurs in situations where the animal can not survive. This robustness supports the differential adhesion hypothesis, while the finite cell mobility accounts for the limit on the spatial range of the sorting.

### 3.1.3. Effect of surface tensions on the minimum energy state

While surface energies determine the local roughness of the energy landscape, and hence the dynamics, the surface tensions conveniently describe the configurations with the absolute energy minimum, i.e. the stable equilibrium states (Fig. 5). In the trivial case where  $\gamma_{dM}$  and  $\gamma_{lM}$  are not positive, cells do not aggregate [Fig. 5(c) and (d)]. More interesting is the miscible case where  $\gamma_{dl}$  is not positive: dark and light cells intermingle [Fig. 5(e)]. For such checkerboard-like patterns experimentally observed in avian oviduct (Honda *et al.*, 1986), surface tension is conventionally said to be zero, but is really undetermined.

In most aggregates, the energy minimum occurs when cell demix to form two homotypic clusters [Fig. 5(f)–(i)]. The surface tensions  $\gamma_{db}$ ,  $\gamma_{dM}$  and  $\gamma_{lM}$  are positive. In the minimum energy configuration the two clusters are in contact together and with the medium. The three interfaces are spherical caps and meet along a triple contact

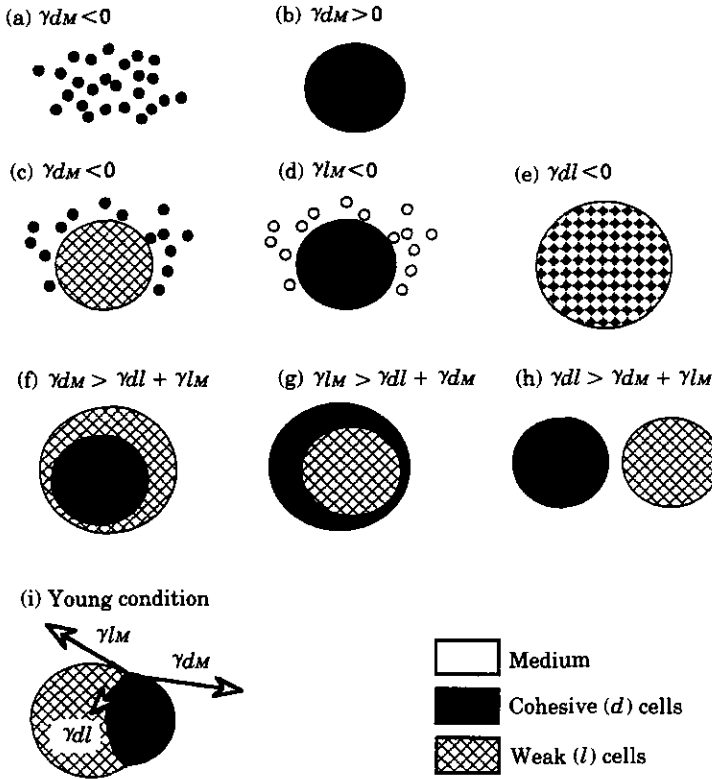


FIG. 5. Surface tensions [eqn (6)] determine the configuration with the minimum global energy. (a) and (b) With one type of cell, two cases occur: dispersal and cohesion. (c)–(e) With two types of cells, and at least one negative surface tension: cells disperse, or mix into a checkerboard. (f)–(h) If one surface tension is greater than the sum of the others, the corresponding interface vanishes at equilibrium. (i) Between these extremes, the three interfaces  $d-l$ ,  $d-M$  and  $l-M$  are stable and meet along a triple contact line. Their three radii are determined by their contact angle and the proportion of dark and light cells. All these configurations are experimentally observed, but (e)–(i) are dependent on initial conditions, and metastable cases also occur (see text).

line. In the plane normal to the edge, the three surface tensions, considered as vectors along the interface, add to zero at equilibrium [Young condition, Fig. 5(i)]. This condition fixes the contact angle; together with the volumes of the two cell clusters, three constraints fix univocally the three radii of the interfaces.

Before equilibrium is reached, the Young condition is not satisfied. Surface tensions simplify the description of the system only when there is much less heterotypic than homotypic interface, which is not the case during the first steps of demixion.

If one surface tension is greater than the sum of the two others, no triple intersection can be stable and the more costly interface disappears [Fig. 5(f)–(h)]. If  $\gamma_{dM} > \gamma_{dl} + \gamma_{lM}$ , (or equivalently  $e_{dM} - e_{dl} > e_{lM} - e_{dl}$ ), dark cells escape from the medium more than light cells. All dark cells leave the free edge of the aggregate, then

cluster within the light cells, a typical cell-sorting case [Fig. 5(f)]. Conversely, as Phillips & Davis (1978) pointed out,  $\gamma_{IM} > \gamma_{dl} + \gamma_{dM}$  would explain a case of position reversal, light cells escaping the free edge and being surrounded by the more cohesive dark cells [Fig. 5(g)].

If  $\gamma_{dl} > \gamma_{dM} + \gamma_{IM}$  (or equivalently  $e_{dl} > e_{dM} + e_{IM}$ ), cell separation is less costly than heterotypic contact [Fig. 5(h)]. Then initially separated clusters remain separated, and initially mixed aggregates disperse into many small homogeneous clusters. This happens if the  $d-l$  interaction is repulsive, but also if it is less attractive than the medium.  $\gamma_{dl}$  is a fine control parameter which selects either dispersal or cohesion, explaining why small qualitative or quantitative changes in adhesion molecules expression yield drastic effects (Mège, 1991).

### 3.1.4. Metastability

Our mobility rule implies that cells are not always able to reach the absolute energy minimum, but can stick in a metastable local energy minimum. *In vivo* cells are not initially mixed, so the *in vitro* initial conditions of cell-sorting can lead to metastable states which are never observed in living organisms, for example, partial cell-sorting or cell dispersal (see above).

Observations of a hydra aggregate cut in ten successive cryosections after 3 days regeneration furnish a three-dimensional reconstruction (Fig. 6; see also Lehn, 1953). In addition to the expected spherical ectoderm–endoderm bilayer, this aggregate possibly displayed an ectoderm cylinder crossing the cavity, covered by a monolayer of endoderm cells facing the cavity liquid. If this reconstruction is correct, it means that this aggregate reached during its cell-sorting phase a configuration topologically equivalent to a torus, which can not decay continuously into a normal sphere-like shell.

Trembley (1744) inverted hydras through their mouths like a glove, with the endoderm monolayer outside and the ectoderm monolayer inside, leaving the mesoglea intact. Although he observed no global reversal, within 24 hr all cell types returned to their normal positions. Probably, the cells intercalated without having to overcome any energy barrier.

Armstrong & Armstrong (1984) observed a metastable mixture of chick embryonic cardiac cells. Mesenchyme (Mes) cells are normally more cohesive than myocardium (My) cells, possibly thanks to a fibronectin-rich extracellular matrix. Aggregation destroys this matrix so that Mes cells are less cohesive ( $e_{\text{Mes-Mes}}$  increases) and sort outwards. They secrete fibronectin at the edge of the aggregate only if in contact with a serum factor contained in the culture medium. Only when all Mes cells are near the edge do they all become cohesive. This reversed aggregate confirms DAH1 but contradicts DAH2. It has reached a local energy minimum, because the surface energies have been continuously changing during the sorting before reaching their normal values. If it is wounded, a My-medium interface forms and progressively extends at the expense of the Mes-medium interface until the aggregate returns to the global energy minimum, which has Mes cells inside and My outside.

Pathological metastable cases have a different topology from stable states.

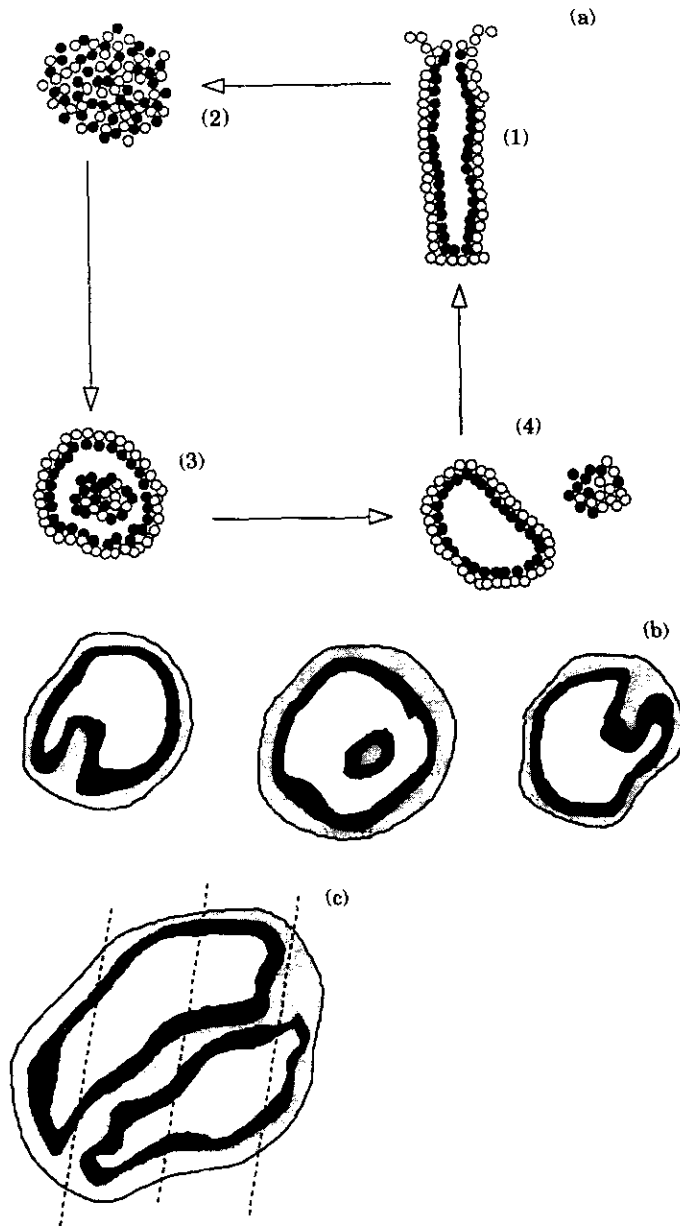


FIG. 6. Experimental observation of a metastable *Hydra* aggregate. From Technau & Graner (unpublished observations). (a) Rough sketch of the aggregation and regeneration of an adult *Hydra* (1). Cells are dissociated, mixed and aggregated (2). Endoderm (dark) and ectoderm (light) epithelial cells undergo cell-sorting within 6 hr, leading to the formation of a bilayer. The aggregate forms a cavity (white) after 18 hr of regeneration (3), expels central cells (4) and begins to reconstruct a head and then an entire normal animal (Noda, 1971; Gierer *et al.*, 1972). (b) Cryo-sections of an aggregate, after 3 days, i.e. well after cavity formation. Of ten equidistant microsections, three, six and nine are sketched here. Lehn (1953) reports a similar observation on an aggregate of *Hydra* tissue fragments. (c) Speculative three-dimensional reconstruction of the aggregate in (b). A cylinder of ectoderm, coated by endoderm, crosses the cavity, which is topologically equivalent to a torus. Dashed lines indicate possible positions of the microsections.

Relaxation towards the global energy minimum is possible only if cells have a channel in the energy landscape (not in the real space) through which they can flow continuously by following an energy gradient.

### 3.2. TEMPERATURE

#### 3.2.1. Statics: how does thermodynamics apply to cell sorting?

Classical equilibrium thermodynamics determines the minimum of the free energy  $F$  for a binary alloy of  $Nx$  atoms of type  $A$  and  $N(1-x)$  of type  $B$  (Reif, 1965). Consider an alloy where the energies  $\varepsilon$  between individuals of the two species  $A$  and  $B$  are such that  $\delta\varepsilon = \varepsilon_{AB} - (\varepsilon_{AA} + \varepsilon_{BB})/2$  is positive. At high temperatures the system is in a disordered, homogeneously mixed phase. At a critical transition temperature  $T_c$  the configuration entropy and interaction energy are of the same order,  $Nk_B T_c \sim N\delta\varepsilon$ . Below  $T_c$  the homogeneous state is stable if one species is rare, but if the initial composition of the mixture is between two critical concentrations  $x_m(T)$  and  $x_M(T)$ , two phases with respective compositions  $x_m$  and  $x_M$  arise. At low temperatures,  $x_m$  and  $x_M$  tend towards 0 and 1, i.e. demixion is complete, minimizing the interaction energy in the absence of an entropy contribution.

However, biological cells contribute to the configuration entropy proportionally to  $N_{\text{cells}}$ . If we assume that specialized molecules are responsible for adhesion,  $\delta\varepsilon$  is of the order of the link energy (1 kcal mol<sup>-1</sup> corresponds to 0.04 eV per link, or  $\delta\varepsilon/k_B \sim 4 \cdot 10^2$  K). The critical temperature is then  $N_{\text{cells}}k_B T_c \sim N_{\text{molec}}\delta\varepsilon$ . If  $n$  is the average number of adhesive molecules per cell,  $n \gg 1$  and  $T_c \sim n\delta\varepsilon/k_B$ . Thus  $T_c$  is many thousands of Kelvin and room temperature corresponds to the very low temperature limit. As far as cell configuration is concerned, the entropy contribution is negligible and there is no point distinguishing energy and free energy. For the temperature range compatible with cell survival, the free energy minimum corresponds to full sorting, as assumed by DAH2.

#### 3.2.2. Dynamics

Such unstable phase-separation, or "spinodal decomposition", occurs in metal alloys, as well as in glasses, liquids and polymer blends (e.g. Gaulin *et al.*, 1987 and references therein).

Thermal agitation drives all the mechanisms by which clusters coalesce or grow: atoms diffuse from one cluster to the other (evaporation–condensation, Lifshitz & Slyozov, 1961), clusters coalesce when bulk or surface atomic diffusion brings them into contact (Binder & Stauffer, 1974; Binder, 1977) or a whole cluster diffuses (Siggia, 1979). Surface tension-driven flow (Siggia, 1979) is rather temperature-independent, and is the only mechanism which can also appear in biological cell-sorting. The aggregate viscosity  $\nu$  is much higher than  $\nu_{\text{water}}$  (Gordon *et al.*, 1972) so the "mesoscopic" cells are too big to diffuse efficiently under thermal agitation.

For Brownian motion (Reif, 1965), a cell with a radius  $R = 10^{-3}$  cm has a diffusion coefficient in water  $D_{\text{water}} = k_B T \rho / 6\pi R \nu_{\text{water}}$  or roughly  $2 \cdot 10^{-14}$  m<sup>2</sup> sec<sup>-1</sup>. This diffusivity is small, 1  $\mu\text{m}$  in 1 min or 25  $\mu\text{m}$  in 10 hr. The diffusion coefficient  $D$  within the

aggregate is orders of magnitude smaller. Thus Brownian motion can barely account for cell-sorting over a few millimeters. However, random temperature-driven local neighborhood exploration could help overcome local energy barriers in metastable states (Graner & Glazier, 1992, 1993) [Fig. 4(b)]. Childress & Percuss (1981) address in detail the mathematical aspect of thermal fluctuations acting on a cell collection.

#### 4. Discussion

##### 4.1. IS THE ANALOGY BETWEEN PHYSICAL AND BIOLOGICAL CELLS LEGITIMATE?

In physical studies of cellular patterns driven by surface tension, we usually quench a system away from equilibrium, then observe its evolution on a slower time scale. In embryology, the genetic regulation of control parameters, such as cell adhesivity, is very slow and cells can rearrange adiabatically. Morphogenesis is a slow cascade of successive quasi-equilibrated states.

However, in cell-sorting we initially dissociate and mix the cells: the aggregate is strongly out of equilibrium. Moreover, its cells do not differentiate much. Although each cell-cell contact becomes more adhesive as more junctions are established, all new cell-cell contacts are identical. In *Hydra* sorting epithelial cells are adult. Their mitotic activity is virtually nil and regeneration produces an animal identical to the initial dissociated adults (Noda, 1971; Gierer *et al.*, 1972; Graf & Gierer, 1980).

The finite size of cells has the following effects:

(i) Cells have a surface, which causes geometrical constraints on cell displacement and intercalation, and also allows a position-dependent surface energy whose gradient acts as a driving force. Sulsky *et al.* (1984) present an evolution equation for an incompressible cellular pattern with a surface energy and derive the Stokes equation for an incompressible fluid. An additional term comes from the cell surfaces; it is non-differentiable, although its one-sided derivatives exist, whenever cells exchange neighbors via a transient four-cell vertex. This singularity is due to cell topology, with no equivalent in hydrodynamics.

(ii) Cells have internal degrees of freedom, on microscopic scales, so that they are highly dissipative. In addition, biological cells can move actively by changing shape. Protrusions and contractions enhance the local exploration of neighboring configurations, but are not necessary for cell-sorting.

(iii) Micrometer-size cells are too big to move and explore ergodically the whole configuration space under thermal agitation. Thus the final state may be a metastable local energy minimum.

##### 4.2. TESTS OF THE HYPOTHESIS

We propose the following approaches to test our cell-cell adhesion hypothesis:

(i) Experimentally, suppress one by one each possible mechanism, including sources of cell motility and cell-cell adhesion. The role of internally generated forces could be assayed by visualizing the distribution of actin components in rearranging

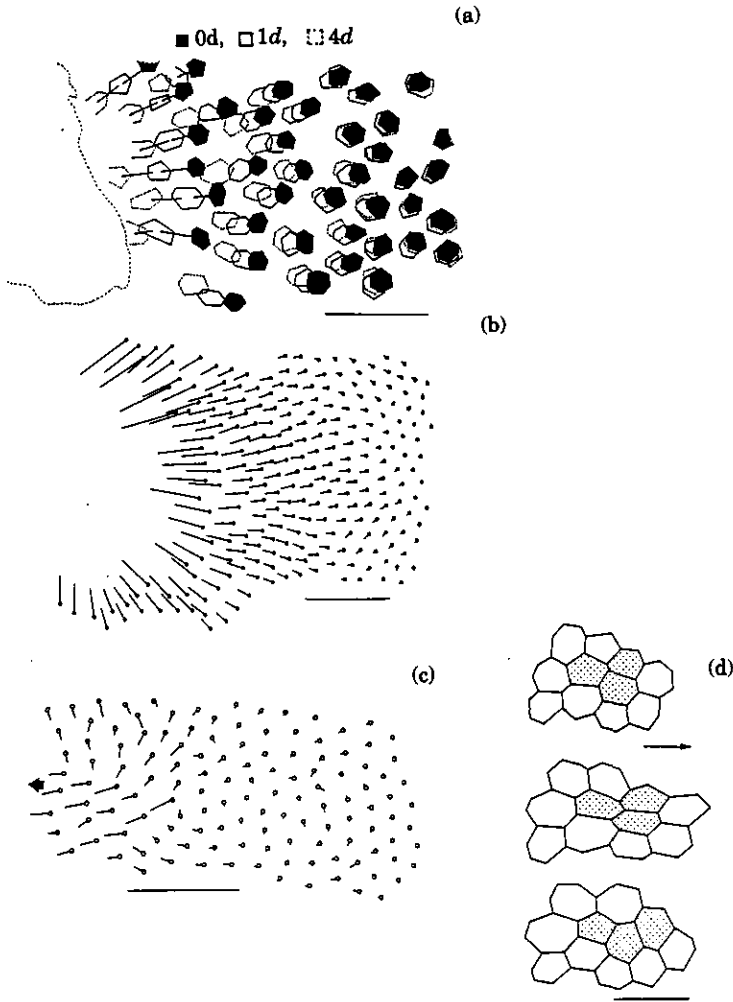


FIG. 7. Experimental observation of cell rearrangement after wounding in cat corneal endothelium. (a) Polygonal cells flatten, migrate and elongate towards the wound (on the left). Solid, full-lined and dotted-lined polygons indicate, respectively, cells just after wounding, and 1 and 4 days later. The bar is 100  $\mu\text{m}$ . (b) Cell movements in the same region. Circles indicate the starting points and segments the displacement during one day. The bar is 100  $\mu\text{m}$ . (c) Cell movements from the 4th to the 12th day. Not all cells move parallel to their neighbors in the direction of the wound, indicated by the arrow. The bar is 100  $\mu\text{m}$ . (d) Neighbor exchange observed near the wound (arrow). Actual cell contours just after wounding, and after 1 and 11 days. The bar is 50  $\mu\text{m}$ . Reprinted from Honda (1983), with permission.

cells (Fristrom, 1988; González & Stidwill, 1991); contractile microfilaments may not be necessary for cell-sorting (Steinberg & Wiseman, 1972). However, inhibition or modification of the expression of adhesion molecules, while leading to drastic effects on cohesion and cell-sorting (Mège, 1991), confirms DAH1 without directly showing that intercellular forces arise from adhesion.

(ii) Measure the cell-cell energy as a function of contact area, to check that a

surface energy really exists (Evans, 1980). Then trace the path followed by each cell during sorting in monolayers and compare it to numerical simulations of adhesion-driven cell movement (Graner & Sawada, 1993).

(iii) Examine cell movements not related to cell-sorting. In homogeneous systems made from only one type of identical cells, the effect of adhesion is simple. Energy gradients arise from inhomogeneities, i.e. from boundaries, and cells rearrange without any potential energy barrier to overcome.

For instance, healing has been observed in cat (Honda *et al.*, 1982) and human (McRae *et al.*, 1986) corneal epithelium (Fig. 7):

(i) Cells at the margin of the wound have a higher apparent velocity.

(ii) All cells seem to move in the same direction at the beginning, then diverge.

(iii) Cells slow, then stop.

(iv) Cell shapes evolve to minimize their membrane length (see Honda, 1983) and are not hexagons.

Honda *et al.* (1982) record changes and contractions in cell shapes "which need not imply contractile activity". If all cells had the same motility (Hardin & Cheng, 1986), (i) and (iii) would be difficult to explain. (ii) indicates that cells do not have access to a positional information (Weliky & Oster, 1990).

Adhesion energy minimization causes each cell to move relative to its neighbors. Here, decreasing the energy reduces both the boundaries of the tissue, and the contact between identical cells. Before wound closure all relative movements have a component towards the wound which geometrically adds to give the impression that marginal cells move faster (i); this global drift slows down (iii) when the wound closes and the relative movements become more apparent (ii). Moreover, (iv) is typical of systems which evolve because of adhesion. The cell-cell contact decreases but does not reach the minimum energy, because hexagonal patterns can be reached only by starting from improbable initial configurations (Herdle & Aref, 1991), or by selective deletion of ill-placed cells as in the fly retina (Cagan & Ready, 1989). Thus, introducing the adhesion amongst other possible driving mechanisms helps explaining even the observed rearrangement of cells of a single type.

## 5. Conclusion

We have shown how either motile or passive cells can sort by following the gradient of surface adhesion energy. Thus adhesion could be not only a guide, accompanying more active mechanisms, but also by itself a driving mechanism for cell rearrangement in both homogeneous and heterogeneous collections of cells.

Our description stresses the difference between biological and physical cellular patterns. The finite size and shape of cells is important. Relating surface tensions to surface energies explains why cell movement stops and metastable states occur in biological experiments. For mixtures of two cell types, the adhesion energy gradient suffices to make clusters of the more cohesive cells coalesce and round.

Such a mechanism does not involve exploratory contacts with distant cells, so internal cell activity is not necessary, although not excluded. It yields a robust dynamical description, broader than existing static ones. It applies to local neighbor

exchange, both in epithelia and in three-dimensional aggregates, and to global cell rearrangement, such as long distance movement in the cell-sorting of heterogeneous aggregates. Moreover, it is compatible with both free and constrained boundaries.

The actual contribution of surface adhesion to cell rearrangement, as compared to the role of other co-operating mechanisms, needs to be tested. However, surface adhesion should not be overlooked when linking morphogenetic phenomena to their molecular explanations. Adhesion-driven dynamics is sufficient to describe biological cell-sorting.

The author would like to thank warmly J. A. Glazier, B. Janiaud, M. Sato and Y. Sawada for valuable help and critical reading of the manuscript, and Ch. González Agosti, H. Honda, U. Technau, P. Tardent and M. Weliky for fruitful discussions. This research has been financially supported by the Inoue Foundation, J.S.P.S., Monbusho.

## REFERENCES

- ARMSTRONG, P. (1989). *Crit. Rev. Biochem. molec. Biol.* **24**, 119–149.
- ARMSTRONG, P. & ARMSTRONG, M. (1984). *J. Cell Sci.* **69**, 179–197.
- BELL, G. (1978). *Science* **200**, 618–627.
- BELL, G. (1979). *Cell Biophys.* **1**, 133–147.
- BELL, G. (1988). In: *Physical Basis of Cell–Cell Adhesion*, Chapter 10 (Bongrand, P., ed.) Boca Raton, FL: CRC Press.
- BINDER, K. (1977). *Phys. Rev. B* **15**, 4425–44470.
- BINDER, K. & STAUFFER, D. (1974). *Phys. Rev. Lett.* **33**, 1006–1009.
- BONGRAND, P. (ed.). (1988). *Physical Basis of Cell–Cell Adhesion*. Boca Raton, FL: CRC Press.
- BORN, G. & PALINSKI, W. (1985). *Br. J. exp. Pathol.* **66**, 543–558.
- BOYLE, R. (1660). *New Experiments, Physico-mechanical, Touching the Spring of Air*. Oxford: Oxford University Press.
- CAGAN, R. & READY, D. (1989). *Develop. Biol.* **136**, 346–362.
- CAPO, C., GARROUSTE, F., BENOLIEL, A.-M., BONGRAND, P., RYTER, A. & BELL, G. (1982). *J. Cell Sci.* **56**, 21–48.
- CARTER, S. (1967). *Nature, Lond.* **213**, 256.
- CHANDRASEKHAR, S. (1961). *Hydrodynamic and Hydromagnetic Stability*. Oxford: Oxford University Press.
- CHILDRESS, S. & PERCUSS, J. (1981). *Lectures on Mathematics in the Life Sciences* **14**, 59–88.
- CURTIS, A. (1988). In: *Physical Basis of Cell–Cell Adhesion*, Chapter 9, (Bongrand, P., ed.) Boca Raton, FL: CRC Press.
- CURTIS, A. & LACKIE, J. (ed.). (1991). *Measuring Cell Adhesion*. England: Wiley.
- DAN-SOHKAWA, M., YAMANAKA, H. & WATANABE, K. (1986). *J. Embryol. exp. Morphol.* **94**, 47–60.
- DAVIS, G. (1984). *Am. Zool.* **24**, 649–655.
- EDELMAN, G. & THIERY, J.-P. (ed.). (1985). *The Cell in Contact*. England: Wiley.
- EVANS, E. (1980). *Biophys. J.* **30**, 265–284.
- EVANS, E. (1983). In: *White Blood Cell Mechanics: Basic Science and Clinical Aspects* (Lichtman, A. & Meiselman, B., eds) p. 53. New York: Alan R. Liss.
- EVANS, E. (1985). *Biophys. J.* **48**, 175 and 185.
- EVANS, E. (1988). In: *Physical Basis of Cell–Cell Adhesion*, Chapters 4 and 7 (Bongrand, P., ed.) Boca Raton, FL: CRC Press.
- EVANS, E. & BUXBAUM, K. (1981). *Biophys. J.* **34**, 1–12.
- EVANS, E. & METCALFE, M. (1984). *Biophys. J.* **46**, 423–426.
- FISCHER, A. (1991). *Médecine/sciences* (in French). **7**, 540–542.
- FOA, C., MEGE, J.-L., CAPO, C., BENOLIEL, A.-M., GALINDO, J.-R. & BONGRAND, P. (1988). In: *Physical Basis of Cell–Cell Adhesion*, Chapter 8 (Bongrand, P., ed.) Boca Raton, FL: CRC Press.
- FRIEDLANDER, D., MÈGE, R.-M., CUNNINGHAM, B. & EDELMAN, G. (1989). *Proc. natn. Acad. Sci. U.S.A.* **86**, 7043–7047.
- FRISTROM, D. (1988). *Tissue Cell* **20**, 645–690.

- GARROD, D. & STEINBERG, M. (1973). *Nature, Lond.* **244**, 568.
- GAULIN, B., SPOONER, S. & MORII, Y. (1987). *Phys. Rev. Lett.* **59**, 668–671.
- GIERER, A., BERKING, S., BODE, H., DAVID, C. N., FLICK, K., HANSMANN, G., SCHALLER, H. & TREKNER, E. (1972). *Nature New Biol.* **239**, 98–101.
- GIUDICE, G. (1962). *Develop. Biol.* **5**, 402–411.
- GLAZIER, J. (1989). *Dynamics of cellular patterns*, Ph.D. Thesis, Chicago, IL: University of Chicago.
- GLAZIER, J. & GRANER, F. (1993). *Phys. Rev. E* **47**, 2128–2154.
- GLAZIER, J., GRANER, F., BERGE, B., MAGNASCO, M., MOLHO, P., FRADKOV, V. & UDLER, D. (1993). *Int. J. Mod. Phys. B*, in press.
- GLAZIER, J. & WEAIRE, D. (1992). *J. Phys. Condens. Matter* **4**, 1867–1894.
- GONZÁLEZ AGOSTI, C. (1985). Diplomarbeit der Universität Zürich (in German, unpublished) and video recordings, available from C. González Agosti.
- GONZÁLEZ AGOSTI, C. & STIDWILL, R. (1991). *Cell Motil. Cytoskel.* **20**, 215–227.
- GORDON, R., GOEL, N., STEINBERG, M. & WISEMAN, L. (1972). *J. theor. Biol.* **37**, 43–73.
- GRAF, L. & GIERER, A. (1980). *Wilhelm Roux Arch. Develop. Biol.* **188**, 141–151.
- GRANER, F. & GLAZIER, J. (1992). *Phys. Rev. Lett.* **69**, 2013–2016.
- GRANER, F. & SAWADA, Y. (1993). *J. theor. Biol.* **164**, 477–506.
- GUSTAFSON, T. & WOLPERT, L. (1963). *Int. Rev. Cytol.* **15**, 139–214.
- HARDIN, J. & CHENG, L. (1986). *Develop. Biol.* **115**, 490–501.
- HERDTLE, T. & AREF, H. (1991). *Phil. Mag. Lett.* **64**, 335.
- HOLTFRETER, J. (1944). *Rev. Can. Biol.* **3**, 220–250.
- HOLTFRETER, J. (1947). *J. Morphol.* **80**, 25–55.
- HONDA, H. (1983). *Int. Rev. Cytol.* **81**, 191–248.
- HONDA, H., OGITA, Y., HIGUCHI, S. & KANI, K. (1982). *J. Morphol.* **174**, 25–39.
- HONDA, H., YAMANAKA, H. & EGUCHI, G. (1986). *J. Embryol. exp. Morphol.* **98**, 1–19.
- HOOKER, R. (1665). *Micrographia*. London, quoted by Glazier 1989.
- JACOBSON, A., OSTER, G., ODELL, G. & CHENG, L. (1986). *J. Embryol. exp. Morphol.* **96**, 19–49.
- KELLER, R. & HARDIN, J. (1987). *J. Cell Sci.* **8**, 369–393.
- KELLER, R. & TRINKAUS, J. (1987). *Develop. Biol.* **120**, 12–24.
- KOLEGA, J. (1986). *J. Cell Biol.* **102**, 1400–1411.
- VAN LEEUWENHOEK, A. (1692). On the formation of rushes. In: *Arcana Naturae, Epistola 74*, quoted by Glazier 1989.
- LEHN, H. (1953). *Roux Archives für Entwicklungsmechanik* **146**, 371–402.
- LEWIS, F. (1948). *Proc. A. A. S.* **77**, 147–186.
- LIFSHITZ, I. & SLYOZOV, V. (1961). *J. Phys. Chem. Solids* **19**, 35–50.
- MCCLAY, D. & ETTENSOHN, C. (1987). *A. Rev. Cell Biol.* **3**, 319–345.
- MCCLAY, D., WESSEL, G. & MARCHASE, R. (1981). *Proc. natn. Acad. Sci. U.S.A.* **78**, 4975–4979.
- MCRÆ, S., MATSUDA, M., SHELLANS, S. & RICH, L. (1986). *Am. J. Ophthalmol.* **102**, 50–55.
- MÈGE, J.-L., CAPO, C., BENOLIEL, A.-M. & BONGRAND, P. (1986). *Cell Biophys.* **8**, 141–160.
- MÈGE, R.-M. (1991). *Médecines/sciences* (in French). **7**, 544–552.
- NEWMAN, S. & COMPER, W. (1990). *Development* **110**, 1–18.
- NICOL, A. & GARROD, D. (1979). *J. Cell Sci.* **38**, 249–266.
- NICOL, A. & GARROD, D. (1982). *J. Cell Sci.* **54**, 357–372.
- NODA, K. (1971). (In Japanese) *Zool. Mag.* **80**, 99–101.
- ODELL, G., OSTER, G., ALBERCH, P. & BURNSIDE, B. (1981). *Develop. Biol.* **85**, 446–462.
- OSTER, G. (1984). *J. Embryol. exp. Morphol.* **83s**, 329–364.
- OSTER, G., MURRAY, J. & HARRIS, A. (1983). *J. Embryol. exp. Morphol.* **78**, 83–125.
- OSTER, G. & PERELSON, A. (1987). *J. Cell Sci.* **8**, 35–54.
- PHILLIPS, H. & DAVIS, G. (1978). *Am. Zool.* **18**, 81–93.
- PHILLIPS, H. & STEINBERG, M. (1978). *J. Cell Sci.* **30**, 1–20.
- PURCELL, E. (1977). *Am. J. Phys.* **45**, 3–11.
- REIF, F. (1965). *Fundamentals of Statistical and Thermal Physics*. New York: McGraw-Hill.
- RELLA, M. (1941). *Roux Archives für Entwicklungsmechanik* **141**, 99–110.
- ROBERSON, M., ARMSTRONG, J. & ARMSTRONG, P. (1980). *J. Cell Sci.* **44**, 19–26.
- SIGGIA, E. (1979). *Phys. Rev. A* **20**, 595–605.
- SMID, I. & TARDENT, P. (1982). *Wilhelm Roux Arch.* **191**, 64–67.
- STEINBERG, M. (1962). *Proc. natn. Acad. Sci. U.S.A.* **48**, 1577–1582.
- STEINBERG, M. (1963). *Science* **141**, 401–408.
- STEINBERG, M. (1964). In: *Cellular Membranes in Development* (Locke, M., ed.) New York: Academic Press.

- STEINBERG, M. (1970). *J. exp. Zool.* **173**, 395–434.
- STEINBERG, M. (1975). *J. theor. Biol.* **55**, 431–443.
- STEINBERG, M. & GARROD, D. (1975). *J. Cell Sci.* **18**, 385–403.
- STEINBERG, M. & WISEMAN, L. (1972). *J. Cell Biol.* **55**, 606–615.
- SULSKY, D., CHILDRESS, S. & PERKUS, J. (1984). *J. theor. Biol.* **106**, 275–301.
- TAKEICHI, M. (1991). *Science* **251**, 1451–1455.
- THOMAS, W. & YANCEY, J. (1988). *Development* **103**, 37–48.
- THOMPSON, D. (1942). *On Growth and Form*, 2nd Edn. Cambridge University Press (Cambridge 1942).
- TREMBLEY, A. (1744). *Mémoires pour Servir à L'Histoire Naturelle d'un Genre de Polypes D'Eau Douce, à Bras en Forme de Cornes*, Leyden.
- VÉLARDE, M. & NORMAND, C. (1980). *Sci. Am.* **243**, 79–93.
- WEAIRE, D., BOLTON, F., MOLHO, P. & GLAZIER, J. (1991). *J. Phys. Condens. Matter* **3**, 2101–2122.
- WELIKY, M. & OSTER, G. (1990). *Development* **109**, 373–386.
- WILSON, H. (1907). *J. exp. Zool.* **5**, 245–258.